AG UPUBLICATIONS





RESEARCHLETTER

10.1002/2017GL073989

Key Points:

- Variation in trench retreat velocity controls the observed slab morphology in lzu-Bonin subduction zone
- The 30 May 2015 Bonin Islands earthquake may be explained as the result of Pacific slab buckling due to slow trench retreat
- Subducted slab is inherently heterogeneous due to nonlinear viscosity, con tributing to the occurrences of isolated deep earthquakes

Supporting Information:

- · Supporting Information S1
- · Movie S1
- Movie S2

Correspondence to:

T. Yang, tyang@gps.ca ltech.e du

Citation:

Ya ng, T., M.Gurnis, and Z. Zhan (2017), Trench motion -<: o ntrolled slab morphology and stress variations: Implkations for the isolated 2015 Bonin Islands deepearthquak, eGeophys. Res. Lett. , 44, 6641-6650, doi:10.1002/2017GI 073989

Received 29 APR 2017 Accepted 14 JUN 2017 Accepted artk le on line 19 JUN 2017 Published on line 3 JUL 2017

Trench motion-controlled slab morphology and stress variations: Implications for the isolated 2015 Bonin Islands deep earthquake

Ting Vang^{1,2} G), Mi chael Gurn is¹, and Zhongwen Zhan¹ G)

'Seismological Laboratory, California Institute of Technology, Pasadena, California, USA, ²Now at School of Earth Sciences, Melbourne University, Melbourne, Victoria, Australia

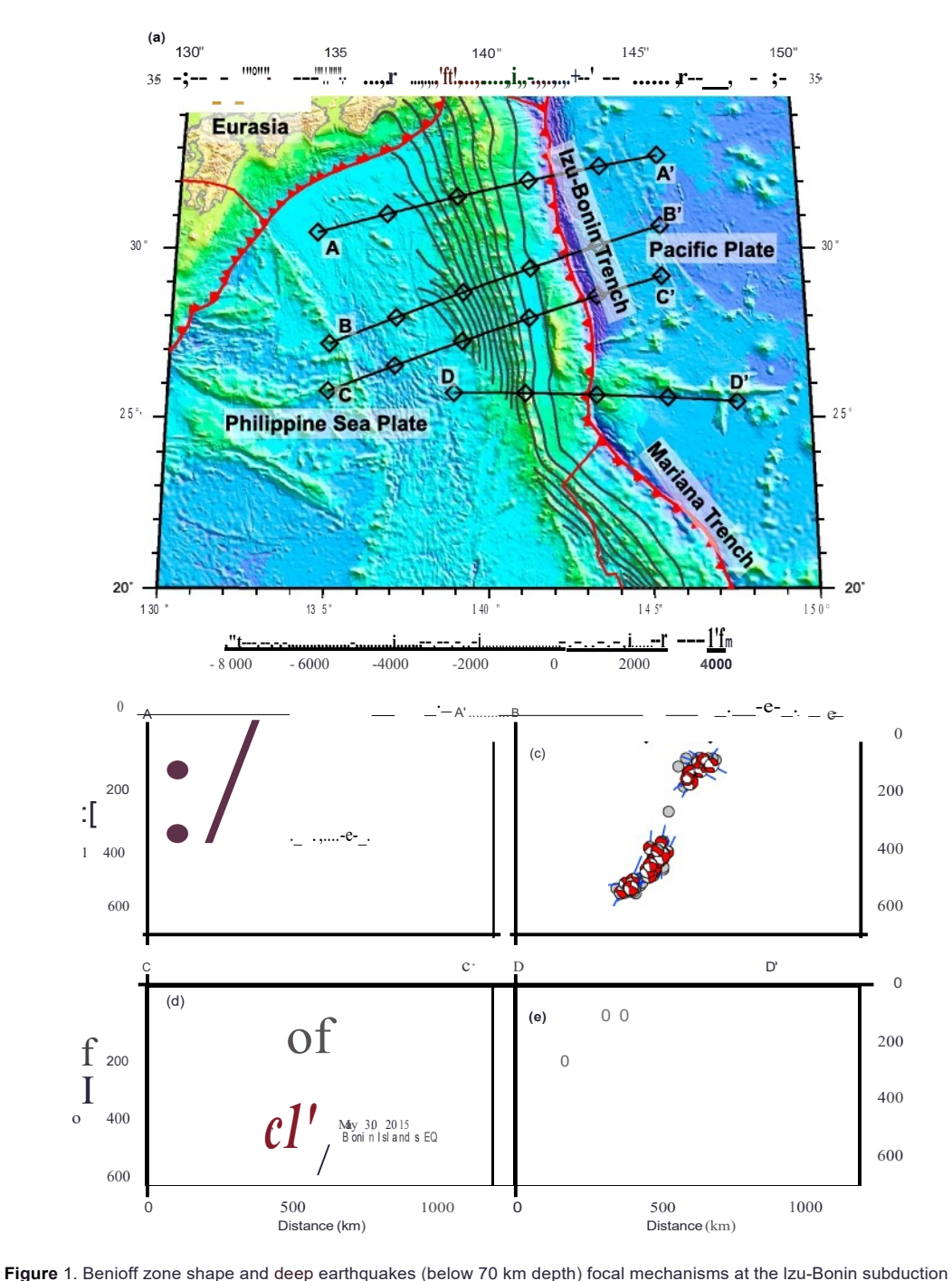
Abstract The subducted old and cold Pacific Plate beneath the young Philippine Sea Plate at the Izu-Bonin trench over the Cenozoic hosts regional deep earthquakes. We investigate slab morphology and stress regimes under different trench motion histories with mantle convection models. Viscosity, temperat ure, and deviatoric stress are inherently het erogeneous within the slab, which we link to the occurrence of isolated earthquakes. Models expand on previous suggestions that observed slabmorphology variations along the Izu-Bonin subduction zone, exhibited as shallow slab dip angles in the north and steeper dip angles in the south, are mainly due to variations in the rate of trench retreat from the north (where it is fast) to the south (where it is slow). Geodynamic models consistent with the regional plate tectonics, including oceanic plate age, plate convergence rate, and trench motion history, reproduce the seismologically observed principal stress direction and slab morphology. We suggest that the isolated -680 km deep, 30 May 2015 *Mw* 7.9 Bonin Islands earthquake, which lies east of the well-defined Benioff zone and has its prin cipal compressional stress direction oriented toward the tip of the previouslydefined Benioff zone, can be explained by Pacific slab buckling in response to the slow trench retreat.

1. Introduction

Subduction of oceanic lithosphere brings cold, high-viscosity material into the higher temperature less viscous mantle. The old and cold Pacific Plate subducts beneath the younger Philippi ne Sea Plate at the Izu-Bonin trench and causes the generation of deep earthquakes (Figure 1). The Wadati-Benioff zone shape varies along the Izu-Bonin subduction zone, IBSZ. The slab dip angle is shallow and the slab flattens at -500 km depth in the northern IBSZ while the slab dip angle is steep in the southern IBSZ (Figure 1). The principal compressional stress direct io n (P axis of earthquake focal mechanism) in the deep continuous part of the slab mainly aligns with the Benioff zone shape, although with significant variations (Figures 1b-le). Consistent with the deep earthquake distribution, tomographic models also indicate that the slab dip angle is small in northern IBSZ and is large in the south [van der Hilst and Seno, 1993; Miller et al., 2005; Wei et al., 2012; Zhao et al., 2017].

On 30 May 2015, a Mw 7.9 earthquake occurred beneath the Bonin Islands at -680 km depth and rupt ured a nearly horizontal plane [Ye et al, 2016]. This event is unusually deep and isolates from the background seismicity forming the Wadati-Benioff zone (Figure I d), presenting an example of an isolated large deep earthquake [Lundgren and Giardini,1994; Frohlich, 2006]. In contrast to previous deep earthquakes regionally that aremainly shallower than 550km, the 2015 Bonin Island earthquake ismuch deeper andlies east of the main trend of the Benioff zone (Figure I d), with its principal compression as tress direction approximately oriented toward thetip of the local Benioff zone [Ye et al., 2016]. It is stillunclear whether this event occurred above or below the 660km discontinuity [Kuge, 2016], which may have been depressed by the cold subducted slab to a depth greater than 680 km [Porritt and Yoshioka, 2016]. Under the implicit assumption that deep earthquakes occur in the cold slab core, Ye et al. (2016] proposed two possible scenarios for the event's large depth and isolation from the Wadati-Benioff zone: (1) a slab tear close to the event separating the gently dipping slab to the nort h and the steeply dipping slab to the south; (2) significant slab folding within the mantle transition due to resistance of the higher-viscosity lower mantle. Oka/ and Kirby (2016) suggested that a previously unknown fragment of fossil slabmaybe responsible forthe surprising eventlocation. On the other hand, based on modeling of strong high-frequency coda waves, Takemura et al. (2016) argued that the Mw 7.9 Bonin earthquake could be located near the bottom edge of the subducted slab, instead of near its center.

02017. Amerkan Geophyskal Union. All Rights Reserved.



zone. (a) Topography [Amante and Eakins, 2009) aroundthe Izu-Bonin subduction zone. Red curved lines represent plate boundaries [Bird, 2003) withsmallred triangles at the subduction zones pointing to the overriding plate. Black curved lines represent slab interface depth from Slab 1.0 model [Hayes et al., 2012). (b-e) Deep earthquake distribution and focal mechanisms at different profiles alongthe Izu-Bonin subduction zone. The profile locations are plotted in Figure 1a. Gray circles represent deep earthquakes from the EHB catalogue [Engdahl et al., 1998). The global centroid moment tensor focal mechanisms are indicative of the 3-Dprincipal stressdirections. Projected compressional axes alongeachprofile(blue line) are also plotted. In Figure 1 d, the 30 May 2015 Bonin Islands deep earthquake is labeled.

Obayashi et al. [2017] proposed a similar explanation that the event occurred near the heelof a boot-like slab structure, before its penetration into the lower mantle. Zhao et al. [2017] suggested that the Pacific slab splits slightly north of the 2015 Bonin earthquake hypocenter which is within the subducting Pacific slab that is penetrating into the lower mantle.

The observed slab {Benioff zone) morphology variations along the IBSZ are qualitatively consistent withslab subduction n umerical models with different trench motion histories. Numerical experiments suggest that trenchmotion history has a significant influence on slab deformation and stagnation within the transition zone [Zhong and Gumis, 1995; Christensen, 1996; Schei/art, 2005; Faccenna et al., 2009; Stegman et al. 2010; Cfikova and Bina, 2013; Agrusta et al., 2017]. The retreat of the trench facilitates slab stagnation within the transition zone, lying subhorizontally. On the other hand, when the trench location is fixed or has a minor retreat with respect to the lower mantle, the slab is more prone to buckle and penetrate into the lower mantle [Christensen, 1996; Cfikova and Bina, 2013]. Although substantial uncertainty exists in the reconstruction of the PhilippineSea Plate region, since it ismostly surrounded by subductionzones, several reconstructions suggest that the northern part of the IBSZ had significant retreat since the Oligocene {~30 Ma}) while southern part of the IBSZ segment had much less retreat during the same period [Hal/, 2002; Miller et al., 2006; Faccenna et al., 2009; Von Hagke et al. 2016; Wu et al., 2016].

We use geodynamic models to investigate slab morphology, temperature, stress regimes and their evolution under different trench motion histories. We demonstrate that models consistent with regional plate tectonics can reproduce the observed slab morphology and deep earthquake P axis directions {assumed to be the principal compressional stress directions} regionally. We suggest that the location of the isolated 2015 Bonin Islands deep earthquake can be explained by the buckling of the Pacific slab beneath the Bonin Islands.

2. Method

We develop a model of plate subduction within a tw<>-<!li>limensional Cartesian geometry and investigate the influences of trench motion history on slab morphology and stress distribution. The equations governing mantle flow with prescirbed initial and boundary conditions are solved with the finite element method using Citcom [Moresi et al., 1996; Zhong, 2006; Lengand Zhong, 2008]. The model domain is set as 2890km in depth (from Earth's surface to core-mantle boundary (CMB)) and 5780 km in width and is divided into 832 equally spaced elements in the horizontal direction (element size 6.95 km) and into 192 uneven elements in the vertical direction. The vertical element size is 5 km in the uppermostmantle and gradually increases to 39.38 km in the lowermost mantle.

The surface is divided intotwoplates with the right old oceanic plate subducts beneath the leftyoung oceanic plate at X = 3800 km {Figure S1 in the supporting information}. Theinitial temperature field is based on a half-spacecooling model (Figures Slb and Slc). The nondimensional temperature boundary conditions at the top and bottom boundaries are O and 1. In contrast to fully dynamic models [Zhong and Gurnis, 1995; Yang et al., 2016], the surface plates and trench motions are prescribed [Chr ist ensen, 1996] so that we can control thesefactors and investigate their influence on slab morphology and stress distribution. Thevelocity of trench retreat is set to the overriding plate velocity.

The viscosity is a composite of dislocation and diffusion creep and depends on depth, temperature, and strain rate [Zhong and Gurnis, 1995; Yang et al., 2016]:

$$q = \frac{100^{\circ}100^{\circ}}{1000^{\circ}}$$

where 11, 'I dif, and 'Idls represent a composite effective viscosity, viscosity via diffusion creep, and viscosity via dislocation creep, respectively. The diffusion creep viscosity is expressed as

'dl |
$$f = 11_0 r(x, z, t) \exp [Eo(To - T) + 1.433 + II.753z - 14.235z2]$$

where 'lo, E_{θ} , and T_{θ} represent no ndimensional viscosity prefactor, activation energy, and referencetemperature in each layer; x, z, t, and T represent nondimensional horizontal and vertical coordinates, time and temperature, respectively. This viscosity setting leads to a high-viscositylithosphere, low-viscosity asthenosphere, viscosity jum p across the 660 km d iscontinuity, viscosity peak at ~2000 km, and gradual viscosity reduction to the CMB {Figure SI) as inferred previously from joint inversion of geophysical observations [*M itrovi ca and Forte*, 2004]. r{ x,z,t) is a weak zone factor [Hebert et al., 2009; Stadler et al., 2010]. The weak zone sits above the subducted slab (Figure SI) and decouples the overriding and subducting plates

[Zhong et al., 1998; van Hunen et al., 2000), mimicki ng the dehyd ration -induced low-viscosity channel and localized sliding along thrust faults between the overriding and subducti ng plates. The weak zone changes its location and shape with time in response to mantle flow.

For simplicity, the nondimensional activation energy of dislocation creep is set to the same as the value for diffusion creep. Thus, the dislocation viscosity can be expressed as follows:

'7dis -
$$\begin{pmatrix} \cdot & 80 \end{pmatrix}$$
 1- $\frac{1}{n}$ 1/n,

where i:11 and i:0 represent the second invariant of the strain rate and the reference strain rate, respectively; and n the nonlinear exponent for dislocation creep. The second invariant of the strain rate eil is defined as

 $eil = \frac{1}{2}(e;x + \pounds;z + 2i;z-)$ In the lower mantle, n is 1 so the lower mantle flow is within the diffusion creep regime. Above 660 km depth, n is 35 so the dislocation creep viscosity is strongly nonlinear. To avoid problems with numerical convergence in response to the imposed surface velocity, n is set to 1 for the top 20 km.

The olivine to spine! phase transition at 410 km and the spine! to perovskite+ magnoustite phase transition at 660km depth are incorporated. The relative density increase at these boundaries is based on preliminary reference Earth mode I [Dziewonski and Anderson, 1981). The Clapeyron slope for the 410 km and 660 km discontinuities are set to 3.0 MPa/K and - 1.5 MPa/K, respectively [Akaogi, 2007; Tauzin and Ricard, 2014). When the temperature is low, the Olivine-spine! phase transition may be delayed, forming a "metastable olivi ne wedge" [Kirby et al., 1996).Metastable olivi ne is incorporated as it may be important for deep earth-quake generation [Kirby et al., 1996; Frohlich, 2006; Zhan, 2017). The setup of the metastable olivine follows previous studies [Schmeling et al., 1999; Yang et al., 2016). Constant parametersused in this paper are listed in Table S1 [Chopelas and Boehler, 1992).

3. Results

In the reference model Case 1 (Table S2 and Figure 2a), the trench retreats rapidly at a velocity of 3 cm/yr. The reference viscosity for this model is 1 x 10^{21} Pa s, corres ponding to a Rayleigh number of 1.075 x 10^8 . The tempe rature, effective viscosity, and stress within the slab are heterogeneous and evolve with time (Figure 2a). The slab dip angle varies with time. After 16 Myr, when the slab reaches and interacts with the 660 km discontinuity, the slab dip angle is shallow and the slab flattens at -500 km and extends westward for several hundred kilometers before it descends again to the bottom of the mantle transition zone. Before the slabreachesthe 660 km discontinuity, the principle compressional stressdirection at intermediate depths (- 200 to -400km depth) ismainly perpendicularto the slab surface, while when the slab reaches the 660 km discontinuity and becomes deflected, along 1 p compresion gradually develops at intermediate depth within the slab (Figure 2a and Video SI), consisted with previous observations and models [/sacks and Molnar, 1971; Vassiliou et al. 1984; Gurnis and Hager, 1988; Alpert et al., 201OJ. The buckling and folding of the slabproducelarge stressinside the slab, consistent withprevious deep earthquake distribution observations [Myhi/1, 2012). Due to the buckling and folding of the slab above the 660km discontinuity, the phase bou ndary beneath the slab is not flat, consistent with recent seismic observations [Gu et al. 2012), and suggests that the stagnant part oft he subducted Pacific platemay not be flat but have small-scaleperturbatio ns. At 16, 21, and 24 Myrs, the shallow slab dip angle, flattened slab at -500 km, and principal stress direction are generally consistent with the seismologic observations at the northern section of the IBSZ (Figures 1b and 1c).

The parametersfor reference model Case 2 (Tabl e S2 and Rgure 2b) are the same as Case 1, except that the trench retreatsat a small,er 1 cm/yr, velocity. Similar to Case 1, the slab temperature, effective viscosity, and stressare heterogeneousand evolve withtime (Figure 2b). Before the slabimpinges upon the 660km discontinuity, the slab dip angle, slab morphology, and principal stress direction withinthe slabare similar to that of Case 1. However, the slab dip angle is generally steep, and the slabcurves towardthe subducting platedirection after the slabinteracts with the 660 km discontinuity in Case 2, in contrast to that of Case 1. At 19 Myrs, the slab morphology and principal stress directions, including the large slabdip angle, the slightly westward extension of the slab at-550 kmdepth, are similar to seismic observations at the southern section of the IBSZ

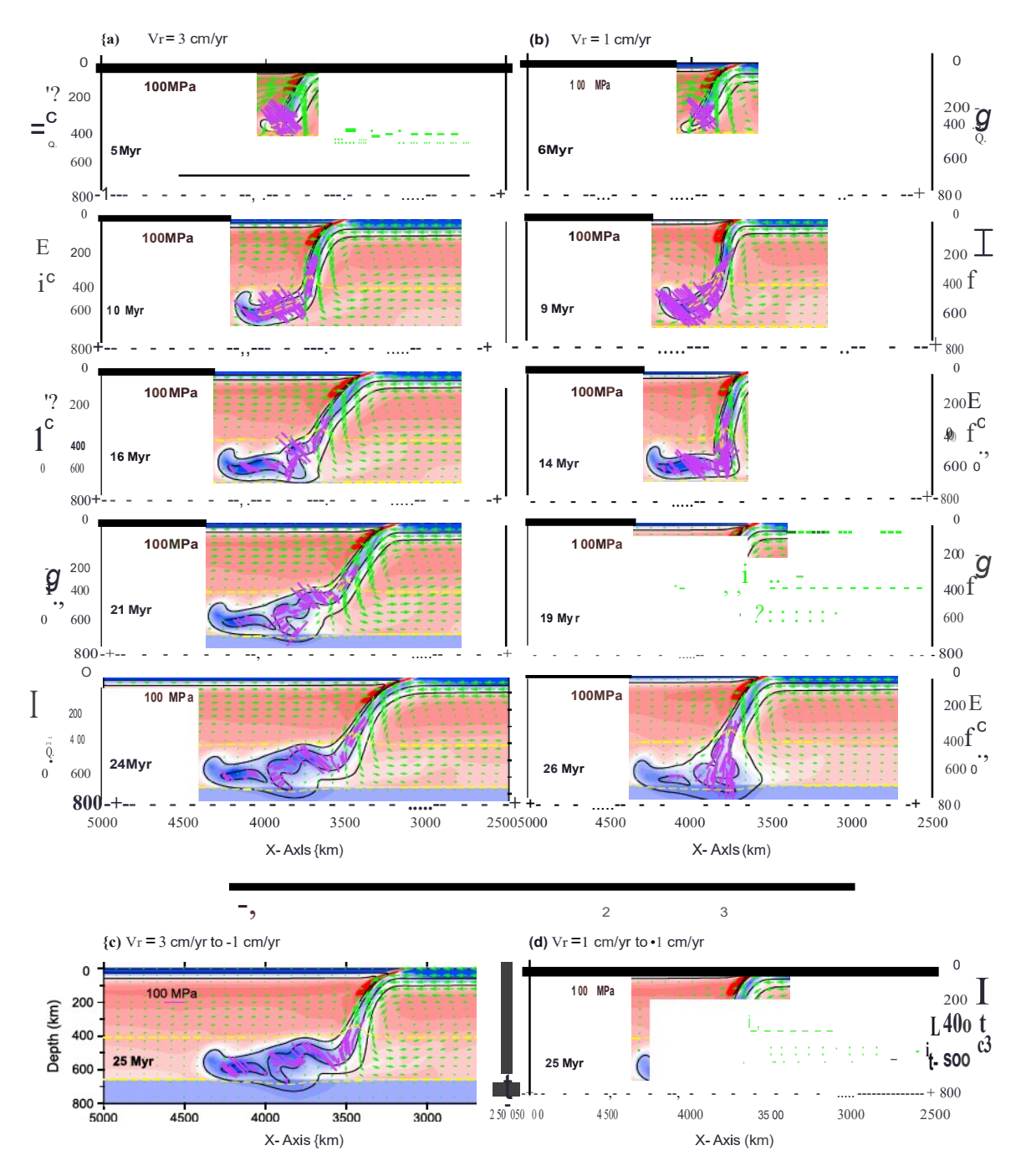


Figure 2. Slab morphology and stress evolution for the reference models (a) Case 1 and (b) Case 2, which have 3 cm/yr and 1 cm/yrtrench retreat velocities, respectively. (c) Case 3 and (d) Case 4 demonstrate the influence of trench advance on slab morphology and stress state at 25 Myr. The background color represents nondimensional viscosity. The 0.6 and 0.8 temperature contours are represented by black lines. We assume that the 0.6 contour represents the cold and strong slab core and the 0.8 contour represents the shape of the cold slab that may be observed by high-resolution seismic tomography. Green arrows represent mantle flow velocity. Purple lines represent principal compressional stress with its length represent stress magnitude. Only a part of the model domain is shown to highlight structures at the subduction zone.

(Figure 1). The slab curves toward the subducting plate direction with its principal compressional stress direction orient ed toward the slab. We link this slab buckling to the isolated 680 km depth Bonin Islands earthquake that lies eastward of the regionally well-defined Benioff zone and has a principal compressional stress pointing toward the predefined Benioff zone tip. Although the low-temperature, high-viscous slab core (represented by the 0.6 temperature contour) has complex buckling within

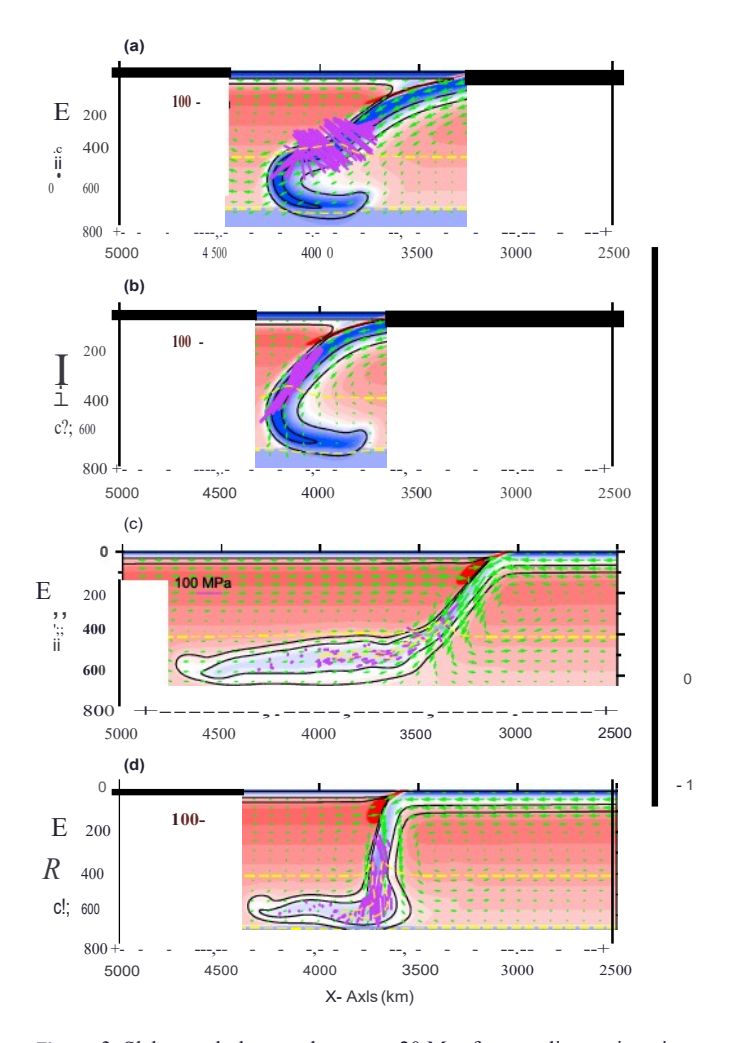


Figure 3. Slab morphology and stress at 20 Myr for pure linear viscosity models. (a) Case 5 and (b) Case6 refer to Case 1 and Case 2, respectively, but considering only linear viscosity. (c) Case 7 and (d) Case 8 refer to Case 5 and Case 6, respectively, but the activation energy is greatly reduced.

the transition zone, the cold slab (represented by the 0.8 temperature contour, which is 27<1'C lower than the surrounding mantle) may only demonstrate a simple geometry (Figure 2b) in smooth tomography models, with the 30 May 2015 Bonin Islands earthquake apparently striking at the heel of the shoe-like cold slab [Takemura et al., 2016; Obayashi et al., 2017].

Although we do not seek a point -bypoint comparison, the general consistency between the simple 2-D geodynamic model s Case 1 and Case 2 and the seismic observations along the IBSZ (Figure 1) is encouraging. Wefurther investigate the influence of recent trench advance [Hall, 2002; Faccenna et al., 2009] on slab morphology and stress state. Case 3 and Case 4 refer to Case 1 and Case 2, respectively, but the trench motion reverses from retreat to a 1 cm/yr advance between 20 and 25 Myrs (Table S2). The change of the trench motion from retreat to advance mainly increases the slab dip angle (Figures 2c and 2d), making models more consistent with seismological observations (Figures1b-1 e).

To investigate the influence of the nonlinear viscosity on slab dynamics, we conducted two models, Case 5

and Case 6 (Figure 3). These two models have the same physical parameters as Case 1 and Case 2,except that only the linear viscosity is considered. The slabs in these linear viscosity models have very higheffective viscosity and less buckling (Figures 3a and 3b). Neither the observed slab morphology nor stress directions are reproduced by these pure linear viscosity models, suggesting that nonlinearviscosity is important in reproducing the observed slab heterogeneity and stress directions. Compared to Case 5 and Case 6, we reduced the activation energy substantially in Case 7 and Case 8 (Figures 3c, 3d,and Table S2). These two weak slab models reproduce the observed slab morphology and stress directions to first order. However, reducing the activation energy in Case 7 and Case 8 greatly reduces the slabviscosity and stress in the flattened section of the slab and may hinder deep earthquake generations there.

Due to the uncertainty in plate reconstruction, we investigated different subducting plate velocity in Case 9-Case 12. Increasing the plate subduction velocity from 6 cm/yr in Case 1 and Case 2 to 8 cm/yr in Case 9 and Case 11 increases the amount of the cold slab embedded into the mantle and increases the degree of slab buckling (Figures4a and 4c).In contrast, reducing the plate subduction velocity to 4 cm/yr in Case 10 and Case 12 reducesthe amount of the coldslabmaterial embedded intothemantle and reduces the degree of slabbuckling (Figures4b and 4d).However, the slabdip angle at shallow depth and principal stress directions are not significantly influenced by subducting plate velocity.

The subducting and overriding plate ages evolve withtime, so weinvestigated the influence of plate ages on slab morphology and stress direction (Case 13-Case 15, Figures 4e-4g). Reducing the overriding plate age

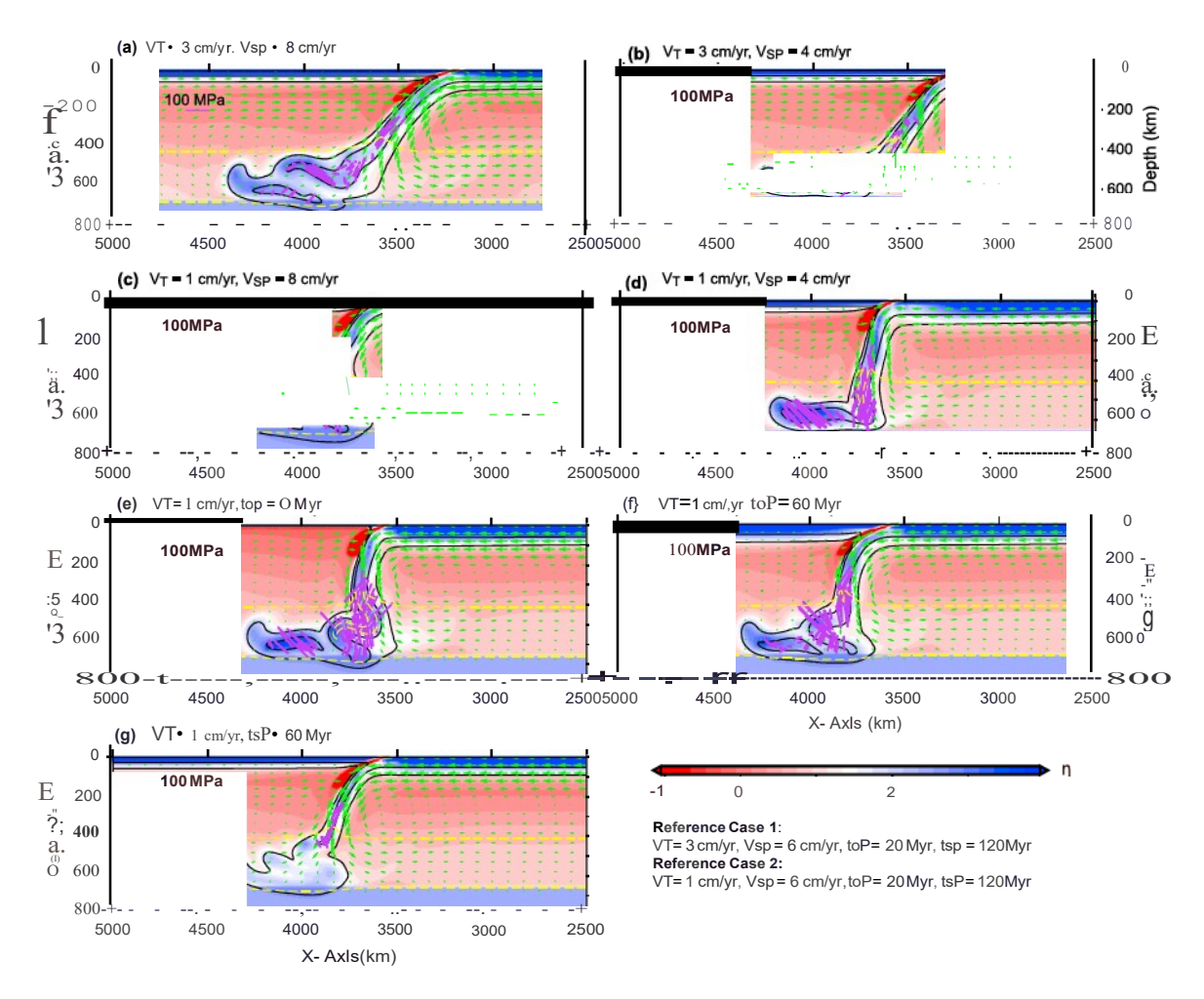


Figure 4. Slab morphology and stress at 20 Myr for different plate tectonics settings. (a-d) Varying t he subducting plate velocity relative to the reference models Case 1 and Case 2. (e-g) Varying the overriding and subducting plate age relative to the reference model Case 2. The parameters of the reference models are labeled at bottom right. The varied parameters of each model relative to the reference models are labeled above each subfigure.

from 20 Myrs in Case 2 to 0 Myrs in Case 13 increases the slab dip angle and reduces the slab temperature with a large metastable olivine wedge developing inside the slab (Figure 4e). In contrast, increasing the overriding plate age from 20 Myrs in Case 2 to 60 Myrs in Case 14 red uces the slab dip angle moderately (Figure 4f), consistent with previous studies [Rodrfgu ez-Gonzdlez et al., 2012]. Reducing the subducting plate age from 120 Myrs in Case 2 to 60 Myrs in Case 15 significantly increases the slab temperature, reduces the stress within the slab, and hinders the generation of deep earthquakes. Infl uences of other physical parameters(activation energy, viscosity jump across the 660 km discontinuity, metastable olivine transitional temperature, and mantle convection Rayleigh num ber) on slab morphology, temperature, and stress distributions can be found in the supporting information.

4. Discussion and Conclusion

We investigated the influence of trench motion velocity on slab morphology and link it with the observed slabmorphology variation alongthe Izu-Bonin subduction zone. Investigations confirm previous suggestions that trench retreat velocity is akeyfactor influencing slab dynamics [Christensen, 1996; Schei/art, 2005; Crikovd and Bina, 2013]. The slab often lies horizontally within the transition zone when the trench retreats rapidly while folding and buckling when the trench retreats slowly [Christensen, 1996; Schei/art, 2005; Faccenna et al., 2009; Crikovd and Bina, 2013; Agrusta et al., 2017]. Comparisons between Case 1 and Case 2 and seismic observations suggestthat the observed slabmorphology variations along thelzu-Bonin subduction zone can be explained by a southward reduction in the trench retreat rate [van der Hilst and Sena, 1993]. However,

self-consistent dynamic models accounting for time-varying trench motion history [Faccenna et al., 2009; Cfikova and Bina, 2015; Yang et al., 2016) are needed in the future.

Zhao et al. [2017) suggested a simple slab geometry with the Pacific slab penetrating into the lower mantle without buckling based on their P wave to mog raphy. In contrast, we suggest slab buckling as the explanation for the 2015 Bonin Islands deep earthquake location and principal stress direction. The horizontal width of the continuous buckling section is usually less than - 300km in our slow slab retreat models (Figures 2b, 2d, and 4), not inconsistent with tomography results [Zhao et al., 2017). Althou gh the slightly westward flattening of the Benioff zone (Figure 1d) gives some support for slab buckling, more seismic in vestigations in regions around the 2015 Bonin Islands earthquake is needed to test the slab buckling model.

Deep earthquakes are oft en regarded as occurring within the cold core of the subducted slabs [KirlJy et al., 1996; Frohlich, 2006), delineating Benioff zones. However, there are occasionally some isolated deep earthquakes that are not obviously connected with any known Benioff zones, although in tomog raphic images, they may lie within high seismic-velocity regions [Engdahl et al., 1995). The mechanism for the formation of these isolated deep events is unclear. We suggest that the slab is essentially heterogeneous, and isolated deep earthquakesmay lie within some isolated cold, strong, and high-stressblocks that are connected with Benioff zones withhigh-temperature and low-viscosity (but may be still colder and more viscousthan the surrounding mant le) belts. Although the stress with in the isolated blocks is usually low (e.g., Figure 2a after 10 Myrs), it may also be high in some cases (e.g., Figures 4e and S2d), providing a natural explanation for the small number of isolated deep earthquakes. Although our modelsdemonstrate the inherent heterogeneity within the subducted slabs, we suggest that the slab heterogeneity would be more obvious when ultrahigh resolution [Gare/et al., 2014) and more real istic rheology are considered.

Our investigation suggests that nonlinear viscosity plays key roles in reproducing the slab heterogeneity and observed stressdirection. When only the linear viscosity is considered, the slab morphology and stressdirection on can only be reproduced by reducing the slab viscosity (activation energy), potentially at least partly explaining the low activation energy and weak slabs previously inferred [Moresi and Gurnis, 1996; Yang and Gurnis, 2016).

Due to the inverse relationship between strain rate (velocity gradient) and viscosity, the high effective viscosity and stressusually correspond to low strain rate. This appears to be contradicted by the occurrence of shallow earthquakesin regions withlargestrain rates(e.g., plate margins). We suggest that the low strain rate only acts to keepthe slab as low tempe rature and high viscosity in the transition zone, while other processe,s e.g., transformati onal faulting, dehydration embritt lement, or shear thermal instability [Frohlich, 2006), act to trigger the deep earthquakes at time scales of seconds to minutes.

Our preliminary investigations demonstrate that geodynamic models consistent with regional plate reconstruction scan reproduce the observed slab stress and morphology variation salong the Izu-Bonin subduction zone, suggesting that plate tectonics and mantle flow over the pasttens of million years controls slab morphology, stress, temperature distributions, and the location and focalmechanism of deep earthquakesin this region. Subduction is essentially 3D with rapid along-trench variations in the Izu-Bonin-Mariana subduction zone (Figure 1). *P* wave tomography suggests that the Pacific Plate splits at - 28°N, slightly north of the 2015 Bonin Islands earthquake [Zhao et al., 2017). That our 2-D model el scan reproduce the observedslab morphology and stressdistribution to the first order suggest that slab tear has limited influenceson deep earthquakes(including the 2015 BoninIslands earthquake) in this region. However, 3-D mant le convection models are needed in the future to bett er understand the influence of along-trench variations and possible tear on slab stressdistribution.

Acknowledgments

T.Y. bene fitted fromthe discussionwith Ling ling Ye. We thank two anonymous reviewers for the ir commentary on the paper. Supported by the NSF under EAR-124702 2, EAR-1600956, and EAR-16 45775. The Finite element software Citcom used for model cakulation can be downloaded from the CIG we bsite https://geod.ynamics.org/.

Referen ces

Agrusta, R., S.Goes, and J.van Hunen (2017), Subducting-slab tr., nsition-zone interaction: Stagnation, penetration and mode switches, Earth Planet. Sci. Lett. 46.4 10 - 23.

Akaogi, M.(2007), Phasetr.,nsitions of minerals in the transition zone and upper part,: Jthe lower mantle, Geo/. Soc. Am Spec. Pop., 421, 1-13, doi:10.1130/2007.2421(01).

Alpert, L, T. Becker, and I. Bailey (2010), Global slabdeformation and centroid moment tensor const@ints on viscosity, Geochem., Geophys., Geosy, st II, Q12006 doi:10.1029/2010GC003301.

Amante, C., and 8. W. Eakins (2009), ETOPOl 1 arc-minute global relief model: Procedures, data sources and analysis, edited, NOAA Tech. Mem. NESDIS NGOC-24, Natl. Geophys. Data Cent, NOAA, doi:10.7289 N SC8276 M.

- Bird, P. (2003), An updated digital model of plate boL11da ries, Grochem., Grophys., Geosyst, 4(3),1027, doi:10.1029/2001GC000252.
- (izkova,,H. and C.R.Bina (201,3) Effects of mantle and subduction-interface rheologieson slab stagnation and trench rollback, *Earth Planet.* Sci. Lett., 379, 95-103, doi:10.1016/j.eps1.2013.08011.
- (izkova, H., and C. R Bina (2015), Geodynamks of trench advance: Insights from a Philipp ine-Sea-style geometry, Earth Planet Sci. Lett., 430, 408-415
- Chopel,as A. and R. Boehle r (1992), The rmal expansivity in the lower mant,le *Grophys. Res. Lett,* 19(19), 1983-1986, doi:10.1029/92GL02144
- Christe nse n, U. R. (1996), The influe nce of trench migration on slab penetration into the lower mantle, *Earth Planet.Sd. Lett*, 140(1), 27-39. Dziewonski, A. M., and D. L. Anderson (1981), Preliminary reference Earth model, *Phys. Earth Planet Inter.*, 25(4), 297-356.
- Engd a,h 1,E. R Vander Hilst, and J. Berrocal (199,5) Imag ing **d** subducted lithosphere beneath South Ameri,ca *Geophys.Res.Le,tt.* 22(16), 2317-2320, doi:10.1029/95GL02013.
- Engd ah l, E.R., R.van der Hilst, and R.Buland (1998), Global telese ismk earthquake relocation with improved trave ltimes and procedures for depth determination *Bull. Seism o/.* Soc. Am, 88(3), 722-743.
- Fæcenna C., E. Di Giuseppe F. Fl. lliciello S. Lallemand and J. Van Hunen (2009), Control of seafloor aging on the migration of the lzu-Bonin-Mariana trench, Earth Planet. Sci. Lett., 288(3), 386-398.
- Frohlkh, C. (2006,) Deep Earthquakes, pp. 252 304, Cambridge Univ. Press, Cambridge, U. K.
- Garel, F., S.Goes, D.Davies, J. H. Davies, S.C. Krame r, and C.R.Wilson (2014), Interact ion of subducted slabswith the mantle transition-zone: A reg ime diagram from 2-Dthermo-mechankal models with a mobile trench and an overriding pla,te *Geochem.*, *Geophys.*, *Gro sy, st 15*, 1739-1765, doi:10.1002/2014GC005257.
- Gu, Y.J. A.Oke ler, and R Schultz (2012), Tracking slabs beneath northwestern Pacific subd uction zones, *Earth Planet. Sci. Lett.*, 331, 269-280. Gurnis, M., and B.H. Hage r (1988), Controls of the structure of subducted slabs, *Nature*, 335(6188), 317-321.
- Hall R. (2002) Cenozok geologk aland plate tectonic evolution of SE Asia and the SW Pacific Computer based reconst ructions, model and an imations, J. Asian EarthSd., 20(4), 353-431.
- Hayes, G. P., D.J. Wald, and R.L. Johnson (2012), Slab1.0:Athree-dimensional model of global subduction zonegeo metries, *J. Grophys. Res.*, 117, BO1302,doi:10.1029/2011JB008524.
- Hebert L.B. P. Antoshec hkina P. Asimo, w and M. Gurnis (2009) Emergence of a low-viscosity channe 1 in subduction zonesthrough the coupling of mantle flow and the rmodynamks, *Earth Planet*. Sd. Lett., 278(3), 243-256.
- Isac ks, B,. and P. Molnar (1971), Distr ibut io n of stresses in the descend ing lithosphere from a global survey off ocal-mechanism solutions of mantle earthquakes, *Rev. Grophys.*, 9(1), 103-174, do i:10.1029/RG009i001p00103.
- Kirby, S.,H. S. Ste,in E.A.Ok,a1 and D.C. Rubie (1996), Metasta ble mantle phasetransformations and deep earthquakes in subducting oceans lithosphere, Rev. Grophys., 34(2), 261-306, doi:10.1029/96RG01050.
- Kug e, K. (2016), The 30 May 2015 Bonin dee p e arthq uake and the 660-km d isco ntinuity around its source region, AGU Ann. Meet. ed ited, San Francisco, Calif.
- Leng, W. and S. Zhong (2008) Viscous heating adiabatic heating and energetic consistency in compressible mantle convection *Grophys.J. Int.* 173(2), 693-702.
- Lundgre n, P., and D.Giardini (1994), Isolate d deepearthquakesand the fate of subduction in the mantle, *J. Grophys. Res.*, 9 9 (B8), 15,833-15,842,doi:10.1029/94JB00038.
- Miller M. A.Gorbato, v. and B.Kennett (2005), Heterogeneity within the subducting Pacific slab beneath the Izu-Bonin-Mariana arc: Evidence from tomography using 3D ray tracing inversion techniques, *Earth Planet. Sd. Lett.*, 235(1), 331-342.
- Mille r, M, B. Kennett, a nd V.Toy (2006), Spatia l and te m po ral evo lution of the subd ucting Pacific plate structure along the western Pacific margin, J. Geophys. Res., 111, B02401, doi:10.1029/2005JB003705.
- Mitroviça, J. and A. Forte (2004), A new inference of mantle viscosity based upon joint inversion of convection and glacial isostatic adjustment data, Earth Planet. Sd.Lett., 225(1), 177-189.
- Moresi, L. and M Gurn is (1996), Constraints on the lateral strength of slabsfrom three-dimensional dynamic flow models, Earth Planet. Sci. Lett., 138(1), 15-28.
- More,si,L S.Zhon,g and M.Gumis (199,6) The acc1Jacy of finite element solutions of Stokes's flowwith strong lyvarying viscosi,ty Phys. *Earth Planet. Inter.*, 97 (1), 83-94.
- Myhill, R (2012), Slab buckling and its effect on the distributions and focal mechanisms of deep-focuse arthquakes, *Geophys. J. Int*, do i:10.1093/gji/ggs1054.
- Obayash, i M. Y.Fukao, and J. Yoshimitsu (2017), Unusua llyd eep Bonin ea rthquake of 30 May 2015: A precursory signal to slab penetration? *Earth Planet. Sd. Lett.*, 459, 221-226.
- Okal, E., and S. H. Kirby (2016), The large Bonin deepeventd 30May 2015: Seismog enesis in a deta ched and fragmented slab, paper presented at EGU Gene ral Assembly Conf. Abstr., Vienna.
- Porr;itt R.W. and S. Yoshioka (2016), Slab pileup in the mantle transition zone and the 30 May 2015 Chichi-jima earthquake *Grophys. Res. Lett.*, 43, 4905-4 912, doi:10.100212016GL068168.
- Rod riguez -Gonza lez, J., A.M. Neg redo, and M. I. Billen (2012), The role of the overriding plate thermal state on slabdip varia bility and on the occurrence of flat subduction, *Grochem, Geophys., Geosyst*, 13, Q01002, doi:10.1029/02011GC003859.
- Schellart W. (2005), Influence of the subducting plate velocity on the geometry of the slab and migration of the subduction hinge Earth Planet. Sci. Lett., 231(3), 197-219.
- Schmeling, H., R Monz, and D.C. Rub ic (1999), The influence of olivine metasta bility on the dynamks of subduction, *EarthPlanet Sd. Lett.*, 165(1), 55-66.
- Stadler G. M. Gum, is C. Burstedde L. C. Wilcox L. Alisic, and 0. Ghattas (2010) The dynamics of plate tector ks and mantle flow. From local to global scales, *Science*, 329(5995), 1033-1038.
- Stegman, D. R.Farrington, F.Capitan io, and W. Schellart (2010J A regime diagram for subduction styles from 3-D numerical models of free subduction, *Tectonophysics*, 483(1), 29-45.
- Takemura ,S. T. Maeda T. Furumura and K. Obara (2016) Constraining the source location of the 30 May 2015 (Mw7.9) Bonin deep-focus earthquake using seismog ram envelopes of high-frequency P waveforms: Occurrence of dee p-focus earthquake at the bottom of a subducting slab, Grophys. Res. Lett., 43, 4297-4302, doi:10.1002/2016GL068437.
- Tauzin, B., and Y.Ricard (2014), Seismka Ily deduced thermodynamics phased iagrams for the mantle transition zone, *Earth Planet Sd. Lett.*, 401 337-346.
- vander Hilst, R., a nd T. Seno(1993), Effects of relative plate motionon the deepstruct ure and penetration depth of slabsbelow the lzu-Bonin and Maria na island arcs, *Earth Planet. Sci. Lett.*, 120(3), 395-407.

Sd. Rep., 7, 44487, doi:10.1038/srep44487.

- van Hunen, J., AP. van den Berg, and N.J. Vlaar (2000), A the rmo-me chanic.al mod el of hor izontal subduction belowan Ollerriding plate, Earth Planet. Sci. Le,tt. 182(,2) 157-169.
- Vassilio u.M., B. Hager, and A. Raefsky (1984), The distribution of earthquakes with depth and stress in sib ducting slabs, *J. Geodyn.*, 1(1), 11-28.
- Von Hag ke, C., M. Philippon, J.-P. Avouac, and M Gumis (2016), Origin and time evolution of subduction polarity reversal from plate kinematics of Southeast As,ia Geology, 44(8),659-662.
- Wei, W. J. Xu, D.Zhao, and Y. Shi (2012), East Asia mantle tomography: New insight into plate subduction and intraplate volc.anism, J. Asian EarthSd., 60, 88-103.
- Wu, J.,J. Suppe, R. Lu, and R. Kan da (2016), Phi lipp ine Sea and East Asian pla te tecton ics since 52 Ma constrained by new subducted slab reconstruction methods *J. Geophys. Res. Solid Earth*, 121, 4670-4741 doi:10.1002/2016JB012923.
- Yang, T. and M.Gumis (2016) Dynamic topography, gravity and the role < i lateral viscosity variations from inversion < i glob al mantle flow, Geophys. J. Int., 207(2), 1186-1202.
- Yang, T, M. Gurnis, and S. Zahirovic (2016), Slab avalanche-induce d tectonics in self-consistent dynamic models, *Tectonoplysics*, doi:10.1016/j.tecto2016.1012.1007.
- Ye, L, T. Lay, Z. Zhan, H. Kanamor i, and J.-L. Hao (2016), The isolated --680 kmdee p 30 May 2018 Mw 7.9 Ogasawara (Bonin) Islands e arthquake, EarthPlanet. Sd. Lett, 433, 169-179.
- Zhan, Z. (2017), Gutenberg-Richter lawfor dee p earthquakes revisited: Adual-mechanism hypothesis, Earth Planet Sd. Lett., 4 61, 1-7. Zhao, D. M. Fujisa wa and G. Toyok., i (2017) Tomography of the subducting Pacific sh b and the 201S Bonin deepest earthq uake (Mw 7.9),
- Zhong, S.(2006), Const raints on thermochemic.al convection of the mantle from plume heat flux, plume excess temperature, and upper mantle temperature, *J.Geophys. Res.*, 111, B04409, doi:10.1029/2008JB003972.
- Zhong S. and M. Gurnis (1995), Mantle convection with plates and mobile faulted plate margins Science 267(519,9) 838.
- Zhong, S., M.Gumis, and L.Mores i (1998), Role of faults, nonlinear rheology, and viscosity structure ingenerating plates from instantaneous mantle flow models, *J. Geophys. Res.*, 103(87), 15,255-15,268, doi:10.1029/98JB0060S.